A Member of a New Class of GTP Cyclohydrolases Produces Formylaminopyrimidine Nucleotide Monophosphates†

David E. Graham, Huimin Xu, and Robert H. White*

Department of Biochemistry, Virginia Polytechnic Institute and State University, Blacksburg, Virginia 24061-0308

Received September 20, 2002; Revised Manuscript Received October 21, 2002

ABSTRACT: The hyperthermophilic euryarchaeon *Methanococcus jannaschii* has no recognizable homologues of the canonical GTP cyclohydrolase enzymes that are required for riboflavin and pteridine biosyntheses. Instead, it uses a new type of thermostable GTP cyclohydrolase enzyme that produces 2-amino-5-formylamino-6-ribofuranosylamino-4(*3H*)-pyrimidinone ribonucleotide monophosphate and inorganic phosphate. Whereas canonical GTP cyclohydrolases produce this formylamino-pyrimidine nucleotide as a reaction intermediate, this compound is shown to be an end product of the purified recombinant *M. jannaschii* enzyme. Unlike other enzymes that hydrolyze the $\alpha-\beta$ phosphate anhydride bond of GTP, this new enzyme completely hydrolyzes pyrophosphate to inorganic phosphate. As a result, the enzyme has a steady-state turnover of 21 min^{-1}, which is much faster than those of canonical GTP cyclohydrolase enzymes. The effects of substrate analogues and inhibitors suggest that the GTP cyclohydrolase and pyrophosphate phosphohydrolase activities occur at independent sites, although both activities depend on Mg^{2+}.

Archaea produce a diverse pool of compounds from ring-opened GTP,[1] including folates (*1*), pterins (methanopterin and molybdopterin) (*2*−*5*), flavins (riboflavin and deazaflavin) (*6*, *7*), and the modified tRNA nucleoside archaeosine (*8*, *9*). These compounds appear to be derived from GTP by a similar first step: a GTP cyclohydrolase enzyme opens the guanine imidazole ring at the 8,9 C−N bond. Although the two characterized *Escherichia coli* enzymes, GTP cyclohydrolases I and II, catalyze mechanistically similar partial reactions, they are not homologous and they use different strategies for catalysis (*10*−*12*). No homologue of any characterized GTP cyclohydrolase enzyme has been identified in the complete genome sequence of the autolithotrophic marine archaeon *Methanococcus jannaschii* (*13*).

GTP cyclohydrolase I (FolE; EC 3.5.4.16) catalyzes the formation of 7,8-dihydroneopterin triphosphate (compound **4**, Scheme 1B), a precursor to tetrahydrofolate and other pteridines (*14*). Studies of the *E. coli* FolE protein suggest that the enzyme uses a zinc-bound water to produce a hydroxyl ion that reversibly opens the imidazole ring of GTP by nucleophilic attack at C-8 (*15*). The intermediate produced by this partial reaction, 2-amino-5-formylamino-6-ribofuranosylamino-4(*3H*)-pyrimidinone triphosphate (Fapy nucleotide triphosphate, compound **2**, Scheme 1B), is rapidly hydrolyzed by FolE to release formate and produce 2,5-diamino-6-ribofuranosylamino-4(*3H*)-pyrimidinone triphosphate (compound **3**, Scheme 1B) (*16*, *17*). The FolE protein subsequently produces dihydroneopterin triphosphate through a slow, multistep series of intramolecular rearrangements (*18*, *19*). Although the complete biosynthesis of dihydroneopterin triphosphate catalyzed by FolE is a slow reaction (with a turnover number of 0.05 s^{-1}), rates for the partial reactions of ring opening and formate release are relatively fast (with respective rate constants 0.9 and 2.0 s^{-1}) (*19*).

GTP cyclohydrolase II (RibA; EC 3.5.4.25) catalyzes the formation of 2,5-diamino-6-ribofuranosylamino-4(*3H*)-pyrimidinone monophosphate (compound **5**, Scheme 1C), a precursor to riboflavin and deazariboflavin (*7*, *20*). This enzyme releases pyrophosphate from GTP and then hydrolytically opens the imidazole ring to form a formylamino-pyrimidine intermediate, 2-amino-5-formylamino-6-ribofuranosylamino-4(*3H*)-pyrimidinone monophosphate (Fapy nucleotide monophosphate; compound **1**, Scheme 1C) (*12*). A third RibA-catalyzed hydrolysis reaction releases formate from Fapy nucleotide monophosphate. Although this reaction appears simpler than that of GTP cyclohydrolase I, it also proceeds slowly with an apparent rate constant of 0.06 s^{-1} (*21*). For this reason, GTP cyclohydrolase II is one of the rate-limiting steps in a fermentation process that uses *Bacillus subtilis* to commercially produce riboflavin (*22*, *23*). Genetic

† This material is based upon work supported by the National Science Foundation under a grant awarded to D.E.G. in 2002 and NSF grant MCB9985712 to R.H.W.

* To whom correspondence should be addressed. Tel: (540) 231-6605. Fax: (540) 231-9070. E-mail: rhwhite@vt.edu.

[1] Abbreviations: APCI, atmospheric pressure chemical ionization; ATP, adenosine 5′-triphosphate; BCA, bicinchoninic acid; DTT, DL-dithiothreitol; EDTA, ethylenediaminetetraacetate; Fapy, formylaminopyrimidine; GTP, guanosine 5′-triphosphate; α,β-methylene-GTP, α,β-methyleneguanosine 5′-triphosphate; β,γ-methylene-GTP, β,γ-methyleneguanosine 5′-triphosphate; GTP-γ-S, guanosine 5′-[γ-thio]-triphosphate; HEPES, *N*-(2-hydroxyethyl)piperazine-*N*′-(2-ethanesulfonic acid); MALDI-TOF, matrix-assisted laser desorption/ionization time-of-flight; MjGC, *M. jannaschii* GTP cyclohydrolase; NADH, β-nicotinamide adenine dinucleotide (reduced); *p*NPP, *p*-nitrophenyl phosphate; PP_i, inorganic pyrophophate (diphosphate); SDS−PAGE, sodium dodecyl sulfate−polyacrylamide gel electrophoresis; TAPS, [(2-hydroxy-1,1-bis[hydroxymethyl]ethyl)amino]-1-propanesulfonic acid; TES, 2-[(2-hydroxy-1,1-bis[hydroxymethyl]ethyl)amino]ethanesulfonic acid; Tris, tris(hydroxymethyl)aminomethane; TSP, [2,2,3,3-$^2H_4$]-trimethylsilylpropionate; XTP, xanthosine ribonucleotide 5′-triphosphate.

10.1021/bi0268798 CCC: $22.00
Published on Web 11/19/2002

Scheme 1: Reactions Catalyzed by (A) MjGC, (B) GTP Cyclohydrolase I, and (C) GTP Cyclohydrolase II Enzymes

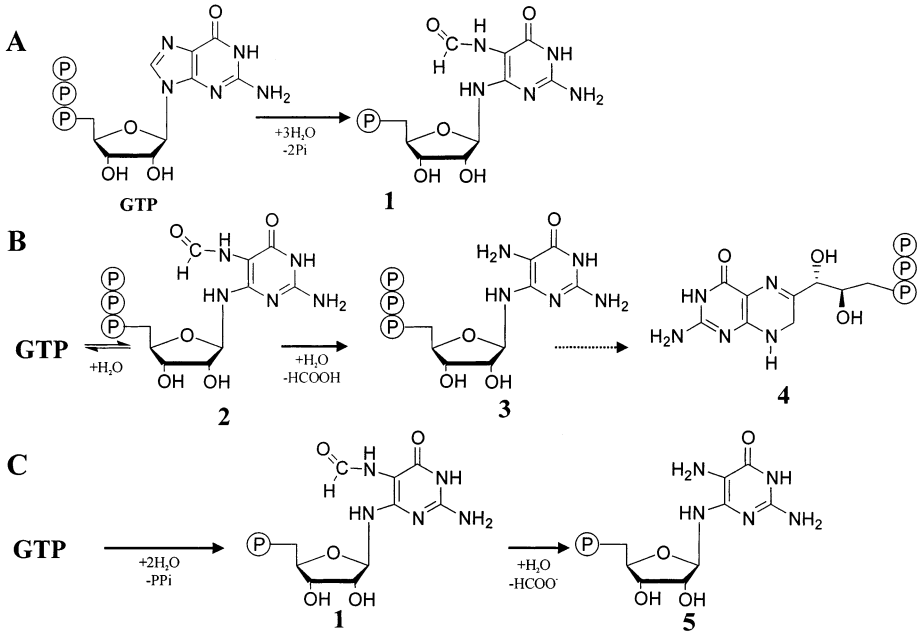

manipulations that increased GTP cyclohydrolase II and 3,4-dihydroxy-2-butanone 4-phosphate synthase activities in *B. subtilis* significantly increased riboflavin titers (*23*).

In this paper we describe the identification and characterization of a new type of GTP cyclohydrolase from *M. jannaschii* that produces 2-amino-5-formylamino-6-ribofuranosylamino-4(*3H*)-pyrimidinone monophosphate (compound **1**, Scheme 1A) and inorganic phosphate. This formylaminopyrimidine product appears to be the starting point for flavin and pteridine biosyntheses in many archaea (White, R. H. (2002) unpublished data). Compared to the *E. coli* GTP cyclohydrolase II, the *M. jannaschii* GTP cyclohydrolase (MjGC) is a fast enzyme, with a steady-state turnover number of 0.35 s^{-1}. The MjGC enzyme represents a new class of GTP cyclohydrolases that couples pyrophosphate hydrolysis to the guanine ring-opening reaction. Members of this class have no recognizable sequence similarity to RibA or FolE proteins.

MATERIALS AND METHODS

Nucleotide Reagents. Xanthosine 5′-triphosphate (XTP) was purchased from Trilink BioTechnologies. 8-Azidoguanosine 5′-triphosphate was purchased from ICN Biomedicals. α,*β*-Methyleneguanosine 5′-triphosphate was prepared from α,*β*-methyleneguanosine 5′-diphosphate and ATP using nucleoside 5′-diphosphate kinase (EC 2.7.4.6) (*24*). The triphosphate product was purified by anion exchange chromatography. Reaction product (100 *μ*L) was loaded onto a Mono Q HR column (5 × 50 mm; Amersham Biosciences) and eluted with a 30 mL linear gradient from 20 to 500 mM ammonium bicarbonate. Fractions containing α,*β*-methylene-GTP were lyophilized to dryness and redissolved in water. 8-Bromoguanosine 5′-triphosphate was prepared by the bromination of GTP (*25*). All other nucleotides were purchased from Sigma-Aldrich. Stock solutions of nucleotide salts were prepared in deionized water. Nucleotide concentrations were determined in phosphate buffered saline solution (pH 7.3) by UV spectroscopy assuming molar extinction coefficients for guanosine nucleotides (13 700 M^{-1} cm^{-1}; 253 nm), inosine nucleotides (12 700 M^{-1} cm^{-1}; 249 nm), adenosine nucleotides (15 400 M^{-1} cm^{-1}; 259 nm), N^7-methylguanosine 5′-triphosphate (8100 M^{-1} cm^{-1}; 258 nm), and 8-bromoguanosine 5′-triphosphate (18 500 M^{-1} cm^{-1}; 262 nm) (*26*−*28*).

Cloning and Recombinant Expression of M. jannaschii GTP Cyclohydrolase in E. coli. The *M. jannaschii* gene at locus MJ0145 (encoding the protein identified by Swiss-Prot accession number Q57609) (*13*) was amplified by PCR from genomic DNA (*29*). Oligodeoxyribonucleotide primer MJ0145-Fwd (5′-GGTGGTCATATGATTCAAATAACAG-3′) introduced an *Nde*I restriction site at the 5′-end of the amplified DNA, whereas MJ0145-Rev (5′-GATCGGATC-CTTAAAACTGTGGATGG-3′) introduced a *Bam*HI site at the 3′-end. DNA fragments were ligated into compatible sites in plasmid pET17b (Novagen). A H136Q mutant of this gene was prepared using the QuikChange site-directed mutagenesis kit (Stratagene) with template pMJ0145 (MjGC in pET17b). The oligodeoxynucleotide primers used for mutagenesis were H136QFwd (5′-GGCTATGTTCAAATCGCT-CAGATAGATATAAACAACATTAC-3′) and H136QRev (5′-GTAATGTTGTTTATATCTATCTGAGCGATTTGAA-CATAGCC-3′). Recombinant plasmids were transformed into *E. coli* BL21-CodonPlus(DE3)-RIL (Stratagene). Sequences of cloned DNA were confirmed by dye-terminator cycle sequencing (University of Iowa DNA Facility). Transformed *E. coli* cells were grown in complex growth medium, and recombinant protein expression was induced with 28 mM α-lactose (*29*). Cells were harvested 4 h after induction by centrifugation (6000 × *g*, 10 min at 4 °C) and were frozen at −30 °C.

Purification of MjGC Protein. *M. jannaschii* GTP cyclohydrolase protein was purified from *E. coli* cells expressing the recombinant MjGC protein. The cell pellet (4.5 g, wet weight) was suspended in 20 mL of 20 mM Tris/HCl (pH 7.6). Cells were lysed by sonication and insoluble material was removed by centrifugation (27 000 × *g*, 15 min at 4 °C). The resulting soluble cell-free extract was heated at 70 °C for 20 min to denature native *E. coli* proteins. After

centrifugation (27 000 × *g*, 15 min at 4 °C), streptomycin sulfate was mixed with the heat-soluble cell-free extract at a concentration of 2.5% (w/v). The mixture was stirred for 7 h at 4 °C before centrifugation (27 000 × *g*, 15 min at 4 °C). The streptomycin-soluble supernatant was placed in an M_r 8000 cutoff membrane (Spectrum) and dialyzed for 12 h at 4 °C in 1 L of buffer containing 20 mM Tris/HCl and 1 mM EDTA (pH 8.0). Dialyzed extract was centrifuged (27 000 × *g*, 15 min at 4 °C), and the soluble portion was applied to a MonoQ HR column (1 × 8 cm; Amersham Biosciences) equilibrated in buffer that contained 50 mM Tris/HCl (pH 8.0). Protein was eluted from the anion exchange column with a 45 mL linear gradient from 0 to 1 M KCl in 50 mM Tris/HCl (pH 8.0) at a flow rate of 1 mL/min. Fractions (1 mL) containing GTP cyclohydrolase activity, which eluted from 400 to 500 mM KCl, were pooled and concentrated in an N_2-pressurized stirred cell with a YM10 ultrafiltration membrane (Millipore).

Concentrated protein was applied to a Sephacryl S-200HR size exclusion column (1.6 × 60 cm; Amersham Biosciences) equilibrated in buffer containing 50 mM TAPS/KOH (pH 8.0) and 150 mM KCl. Chromatography was performed in this buffer at a flow rate of 0.5 mL/min, and GTP cyclohydrolase activity eluted maximally at an elution volume of 49 mL. Fractions containing significant activity were pooled and concentrated by centrifugal ultrafiltration using a Centricon YM-10 device (Millipore). Concentrated protein was stored at 4 °C. The MjGC H136Q mutant protein was purified by the same procedure.

Protein purity was evaluated by SDS−PAGE with silver diamine staining. The size of the denatured protein was analyzed relative to low molecular weight protein standards (Bio-Rad) separated on a SDS−polyacrylamide gel (12%T, 2.7%C acrylamide) with a Tris/glycine buffer system. Protein mass was determined using matrix-assisted laser desorption/ionization time-of-flight (MALDI-TOF) mass spectrometry, as described previously (*30*). Purified MjGC protein (0.5 μL of a 0.7 mg/mL solution) was mixed with 0.5 μL of a 3,5-dimethoxy-4-hydroxycinnamic acid matrix solution on a stainless steel target. Ions of sodium, matrix, bovine pancreas insulin chain B (oxidized), horse heart cytochrome *c*, and bovine serum albumin were used for mass calibration. The hydrodynamic radius of the MjGC protein in its native conformation was analyzed by analytical size exclusion chromatography using a Superose 12HR column (1 × 30 cm; Amersham Biosciences), operated and calibrated as described previously (*29*). Protein concentrations were measured using the BCA total protein assay (Pierce) with bovine serum albumin as a standard.

Identification of the MjGC Nucleotide Reaction Product. The reaction product of MjGC enzyme incubated with GTP was purified by anion exchange chromatography with an ammonium bicarbonate elution gradient as described above for nucleotide purification. The isolated product was diluted to a concentration of 50 ng/μL in 50% (v/v) acetonitrile for analysis by electrospray mass spectrometry using atmospheric pressure chemical ionization (APCI) to obtain a negative ion spectrum (*31*). ^{1}H NMR and ^{31}P NMR analyses were performed at 25 °C using a Varian Inova 400 MHz spectrometer at the Analytical Services facility in the Virginia Polytechnic Institute and State University Department of Chemistry. Purified reaction product was lyophilized to dryness and redissolved in D_2O. Proton resonances were measured relative to an internal [2,2,3,3-$^2H_4$]-trimethylsilylpropionate (TSP) standard ($\delta = 0$). ^{31}P resonances were measured relative to an external H_3PO_4 (85% w/v) standard (0 ppm).

A fluorescent pterin derivative of the reaction product was prepared by the Gabriel-Isay reaction in which a 6-hydroxy-2,4,5-triaminopyrimidine (formed by acid-hydrolysis) is condensed with 2,3-butanedione (*32*, *33*). For hydrolysis, a 50 μL volume of reaction product (in a 1.5 mL polypropylene microcentrifuge tube with a locking lid (Fisher)) was mixed with 50 μL of 1 M HCl and incubated at 95 °C for 5 min. To the cooled sample was added 50 μL of 1 N NaOH and 83 μL of derivatization reagent containing 0.9 M Tris/HCl (pH 8.5) and 34 mM 2,3-butanedione. The reaction was incubated at 95 °C for 45 min. The pterin derivative was analyzed by HPLC and fluorescence spectroscopy. HPLC analysis of the 2,3-butanedione derivative was performed using a C-18 reversed phase column (AXXI Chrom ODS, 5 micron, 23 cm) with a sodium acetate/methanol linear elution gradient, as described previously (*34*). The eluent was monitored for fluorescence using excitation and emission wavelengths of 365 and 445 nm. Fluorescent excitation and emission wavelength maxima were measured in a methacrylate cuvette using a PerkinElmer Life Sciences 650-40 fluorescence spectrophotometer. Using the reaction conditions described above, samples containing 0.5−15 nmol 6-hydroxy-2,4,5-triaminopyrimidine in 5 mM DTT reacted quantitatively with 2,3-butanedione to produce 6,7-dimethylpterin, measured by fluorescence spectroscopic comparison with a standard solution of 6,7-dimethylpterin (emission and excitation wavelengths of 358 and 448 nm). DTT (or 2-mercaptoethanol) was required to minimize the spontaneous oxidation of 6-hydroxy-2,4,5-triaminopyrimidine (*20*).

Analysis of Enzymatic GTP Cyclohydrolase Activity. One unit of GTP cyclohydrolase activity converts 1 μmol/min GTP into formylamino-diaminopyrimidine (Fapy) ribonucleotide monophosphate. Standard activity assays included 50 mM TAPS/KOH (pH 8.0), 50 mM NH_4Cl, 10 mM $MgCl_2$, 5 mM DTT, and enzyme in 50 μL. Assay mixtures were preincubated at 70 °C for 10 min before the addition of GTP (100−150 nmol in 1−2 μL). After 10 min of incubation at 70 °C, activity was terminated by the addition of 50 μL of 1 M HCl. Reaction product was hydrolyzed and derivatized with 2,3-butanedione as described above. Fluorescence of the 6,7-dimethylpterin derivative was measured as described above and 6,7-dimethylpterin concentrations were calculated using the linear regression results from a standard curve of 0−12 nmol of 6,7-dimethylpterin prepared from 6-hydroxy-2,4,5-triaminopyrimidine and 2,3-butanedione.

The same assay was used to measure specific activities of the MjGC enzyme acting on substrate analogues that form a Fapy nucleotide monophosphate product. The rate of N^7-methyl-GTP hydrolysis was measured at 60 °C using UV spectroscopy to detect the increase in absorbance at 270 nm due to the formation of the ring-opened product (*28*).

Analysis of Pyrophosphate Phosphohydrolase Activity. One unit of pyrophosphate phosphohydrolase (inorganic diphosphatase) activity converts 1 μmol/min inorganic pyrophosphate (PP_i) into orthophosphate. Standard activity assays included 50 mM TAPS/KOH (pH 8.0), 50 mM NH_4Cl, 10 mM $MgCl_2$ and enzyme in 50 μL. Assay mixtures

were preincubated at 70 °C for 10 min before the addition of PP_i (250 nmol in 2.5 μL). After 10 min of incubation at 70 °C, activity was terminated by the addition of 650 μL of chilled stop solution containing 2 mM EDTA (pH 8.0). Inorganic phosphate was quantified by the malachite green dye-enhanced phosphomolybdate assay (*35*, *36*). In this assay, inorganic phosphate in a volume of 700 μL is mixed with 300 μL of a freshly prepared solution containing 1.2 M H_2SO_4, 16 mM $(NH_4)_6Mo_7O_{34}$, 0.3 mM malachite green, and 0.15% (v/v) Tergitol NP-10. After 10 min incubation at room temperature, the reactions' absorbances are measured at 610 nm. Inorganic phosphate concentrations were calculated using linear regression results from a standard curve consisting of 0−6 nmol K_2HPO_4 in 700 μL H_2O. Measurements of phosphate from reactions incubated without enzyme were subtracted from measurements of enzymatic reactions to produce the reported values.

Analysis of GTP Pyrophosphatase, GTP Phosphohydrolase, and Alkaline Phosphatase Activities. Pyrophosphate released from GTP during incubation with MjGC was measured using a coupled-enzyme assay in a pyrophosphate reagent kit (Sigma) according to the manufacturer's instructions. The putative pyrophosphatase reaction (in 120 μL) contained 50 mM TAPS/KOH (pH 8.0), 25 mM NH_4Cl, 10 mM $MgCl_2$, 5 mM DTT, 3 mM GTP, and 20 μg MJ0145. After 30 min incubation at 70 °C, this reaction was terminated by the addition of EDTA (10 mM final concentration) and cooled on ice. Aliquots of the reaction or $Na_4P_2O_7$ standard solutions (0−50 nmol PP_i) were added to pyrophosphate assay mixtures preincubated at 30 °C, and the oxidation of NADH was by monitored measuring decreases in absorbance at 340 nm. Pyrophosphate standards were subsequently added to reactions with no net decreases in absorbance to test for inhibitory factors. Inorganic phosphate produced by GTP phosphohydrolase activity was measured using the malachite green phosphomolybdate assay. Alkaline phosphatase activity was measured in reactions containing 50 mM glycine/NaOH (pH 9.5), 5 mM $MgCl_2$, 0.5 mM $Zn(OAc)_2$, and 5 mM *p*-nitrophenyl phosphate (*p*NPP) incubated at 37 °C (*37*). Purified MjGC was added to the solution, and hydrolysis of *p*NPP was monitored by measuring changes in absorbance at 405 nm. Bacterial alkaline phosphatase was used as a positive control.

Cation, pH, Reductant, and Temperature Effects on MjGC Activities. Reaction conditions for MjGC GTP cyclohydrolase activity were optimized by varying components of the standard assay mixture. All reactions were carried out under enzymatic activity-limited conditions. Salts of monovalent cations that were tested as activators of MjGC included LiCl (100 mM), NaCl (100 mM), KCl (50−200 mM), KOAc (50−100 mM), NH_4Cl (25−250 mM), or NH_4OAc (50 mM). Spermidine•3HCl was also tested as an activator at a 10 mM concentration. Divalent metal cation requirements were tested using reagents and enzyme purified by passage through a Chelex 100-K^+ column (1 × 9 cm; Bio-Rad) (*38*). Concentrations of GTP and MjGC reagents were measured by their absorbances at 253 and 280 nm, respectively. Divalent metal replacement reactions included $MgCl_2$•$6H_2O$ (1−6 mM), $MnCl_2$•$4H_2O$ (5 mM), $CaCl_2$•$6H_2O$ (5 mM), $NiCl_2$•$6H_2O$ (5 mM), $ZnSO_4$ (5 mM), $BaCl_2$•$2H_2O$ (5 mM), $CuCl_2$ (5 mM), $CoCl_2$•$6H_2O$ (5 mM), or EDTA. Buffers tested at a final concentration of 50 mM included HEPES/KOH (pH 7.1−7.6), TES/KOH (pH 7.1−8.0), Tris/HCl (pH 8.0), triethanolamine (pH 8.0), and TAPS/KOH (pH 8.0−9.0). The reductants dithiothreitol (10−100 mM), 2-mercaptoethanol (10−100 mM), and dithionite (100 mM) were also tested in MjGC reactions. Effects of reaction temperature were studied in standard assays initiated by the addition of 2.6 mM GTP or 5 mM PP_i. Reactions were incubated from 4 to 94 °C for 10−30 min and then terminated and analyzed according to the standard assay methods.

Steady-State Kinetic Analyses of MjGC activities. For both GTP and PP_i substrates initial reaction rates were measured in standard assays containing 15−20 μg/mL MjGC and various substrate concentrations. Reactions were incubated at 70 °C for 5 min and then terminated and analyzed according to standard assay methods. A curve from the Henri-Michaelis-Menten equation was fit through the GTP cyclohydrolase initial rate data using parameters calculated by the Levenberg−Marquardt method of nonlinear least squares regression (Sigma Plot 2000, SPSS Science). Initial rates of pyrophosphate phosphohydrolase activity were fitted to a simple model for substrate inhibition: $v = V \cdot A/((K_M + A + A^2)/K_i)$ (*39*).

GTP Cyclohydrolase and PPi Phosphohydrolase Inhibitors and Analogues. Potential inhibitors of MjGC GTP cyclohydrolase activity were tested in reactions (50 μL) containing 60 μM GTP, 5 mM DTT, 10 mM $MgCl_2$, 50 mM TAPS/KOH (pH 8.0), 50 mM NH_4Cl, and 0.75 μg MjGC. Reactions were incubated at 70 °C and terminated after 4 min as described for standard cyclohydrolase assays. Potential inhibitors of MjGC PPi phosphohydrolase activity were tested in reactions (50 μL) containing 60 μM sodium pyrophosphate, 10 mM $MgCl_2$, 50 mM TAPS/KOH (pH 8.0), 50 mM NH_4Cl, and 0.9 μg MjGC. Reactions were incubated at 70 °C and terminated after 5 min as described for standard phosphohydrolase assays. Analogues were tested as alternative substrates in reactions without GTP or PP_i, and products were analyzed by anion exchange chromatography (nucleotides) or malachite green phosphate assay (phosphate anhydride compounds).

RESULTS

Identification of MjGC. Although the complete genome sequences of several methanogens encode no recognizable homologues of previously characterized GTP cyclohydrolase genes (*13*, *40*, *41*), these archaea synthesize riboflavin, coenzyme F_{420}, and methanopterin de novo from GTP (*2*, *3*, *6*, *7*). Therefore, we hypothesized that they have novel GTP cyclohydrolase enzymes and that the respective genes could be clustered with other genes required for the biosyntheses of these coenzymes (*42*, *43*). The *Methanobacterium thermoautotrophicum* ΔH genome contains two contiguous genes (*cofD* and *cofE*) that are both involved in coenzyme F_{420} biosynthesis (*40*, *44*, *45*). An adjacent member of this gene cluster, the gene at locus MTH1017, is an ortholog of the *M. jannaschii* gene at locus MJ0145. We cloned this gene from *M. jannaschii* and expressed the MJ0145 gene in *E. coli* for purification and in vitro analysis of GTP cyclohydrolase activity.

Purification of MjGC Protein. Recombinantly expressed MjGC comprised 25% of the *E. coli* cell's total soluble protein. Treating the cell extract by heating, streptomycin precipitation of nucleic acids, strong anion exchange chro-

Table 1: Purification of *M. jannaschii* GTP Cyclohydrolase from Recombinant *E. coli* Cell Paste (4.5 g)

purification step	volume (mL)	total protein[a] (mg)	total activity[b] (units)	specific activity (units/mg)	Yield (%)
soluble extract	19	334	32	0.09	100
heat treatment	19	191	33	0.17	104
streptomycin treatment	16	148	36	0.24	113
MonoQ pool	10	68	25	0.37	79
Sephacryl pool	11	46	18	0.39	56

[a] Total protein was measured using the BCA assay. [b] GTP cyclohydrolase activity was quantified by measuring the fluorescence of the 2,3-butanedione derivative, as described in the Materials and Methods section. One unit of GTP cyclohydrolase activity converts 1 μmol/min GTP into formylamino-diaminopyrimidine ribonucleotide monophosphate.

matography and gel filtration chromatography purified MjGC from any detectable protein or nucleic acid contaminants. Table 1 shows the purification of 46 mg of MjGC protein from 4.5 g of recombinant *E. coli* (wet mass). After concentration by ultrafiltration, the protein was stored at a concentration of 19 mg/mL and had a specific GTP cyclohydrolase activity of 0.43 U/mg. The enzyme retained more than 80% activity after storage for 9 weeks at 4 °C in 50 mM TAPS/KOH (pH 8) and 150 mM KCl.

Purified MjGC preparations showed a single band on a silver-stained SDS−polyacrylamide gel with an apparent molecular mass of 37,000 Da. Analysis of the MjGC protein using MALDI-TOF mass spectrometry identified an ion $m/z = 30\,359 \pm 114$ (MH^+) that is consistent with the protein's predicted molecular mass of 30 275 Da. When loaded on an analytical size-exclusion column, MjGC eluted with a Stokes radius of 38.6 Å, corresponding to an apparent molecular mass of 98 300 Da. This protein's elution profile suggests that MjGC forms a trimer in its native conformation. Measured in phosphate-buffered saline (pH 7.4), MjGC has a single UV absorbance maximum at 277 nm and an extinction coefficient (ϵ_{280}) of 0.7 mL/mg/cm.

MjGC Catalytic Activities and Nucleotide Reaction Products. To detect the expected hydroxytriaminopyrimidine nucleotide product of GTP cyclohydrolase II, MjGC protein was incubated with GTP and then the reaction was heated with 2,3-butanedione to form fluorescent 6,7-dimethylpterin by the Gabriel-Isay reaction (*32*, *33*). Although only trace amounts of fluorescent product were detected from these reactions, a substantial amount of fluorescent material was observed when an acid hydrolysis step preceded the derivatization reaction. The fluorescent product has an excitation maximum at 360 nm and an emission maximum at 448 nm. Analysis by HPLC with fluorescent detection showed that the derivative coeluted with a 6,7-dimethylpterin standard. This result suggested that the reaction catalyzed by MjGC produces a formylaminopyrimidine nucleotide similar to that produced by the His^{179}Ala mutant of *E. coli* GTP cyclohydrolase I (*46*).

The product of the MjGC-catalyzed reaction was purified by anion exchange chromatography; analyses using UV−vis, APCI-MS, ^{1}H NMR, and ^{31}P NMR spectroscopies supported the identification of the reaction product as 2-amino-5-formylamino-6-ribofuranosylamino-4(*3H*)-pyrimidinone monophosphate (Fapy nucleotide monophosphate). UV−vis spectroscopic analysis of the reaction product (in 100 mM sodium phosphate, pH 6.8) identified an absorbance peak at 273 nm with a molar extinction coefficient (ϵ_{274}) of 15 780 M^{-1} cm^{-1}, based on a comparison of fluorescence from the acid-hydrolyzed, 2,3-butanedione derivative to a standard curve of 6,7-dimethylpterin prepared from 6-hydroxy-2,4,5-triaminopyrimidine. APCI-MS operated in negative ion mode detected a deprotonated molecular ion at $m/z = 380$ $(M-H)^-$ from the sample, consistent with the predicted neutral mass for Fapy nucleotide monophosphate of 381.21 Da. ^{1}H NMR (D_2O, 400 MHz, TSP) identified signature resonances corresponding to four isomers of the 5-formylamino compound, similar to those previously described for α and β anomers of the *cis* and *trans* amide bond isomers of Fapy nucleotide triphosphate and model compounds (*46*−*48*): δ 8.293 (1H, s, α-*cis*-CHO, 41% total), 8.265 (1H, s, β-*cis*-CHO, 47% total), 7.911 (1H, s, β-*trans*-CHO, 5.5% total), 7.880 (1H, s, α-*trans*-CHO, 6% total), 5.932 (1H, d, α-*cis* H-1′, $J = 3.2$ Hz, ∼48% total) and 5.715 (1H, d, β-*cis* H-1′, $J = 6.0$ Hz, ∼52% total). The β-*cis*-5-formylamino isomer is the most likely product of MjGC—it is the predominant form of the purified Fapy nucleotide monophosphate, and its resonance is the first to appear in a ^{1}H NMR analysis of GTP incubated with MjGC (data not shown). A ^{31}P NMR spectrum showed two peaks: a broad peak corresponded to the isomers of a nucleotide monophosphate ester and a narrow peak corresponded to inorganic orthophosphate that co-purified with the Fapy nucleotide monophosphate. ^{31}P (^{1}H decoupled) NMR (D_2O, 162 MHz, 85% H_3PO_4 reference) peaks were δ 3.807 (α-mono-P, bs) and 2.389 (P_i, s). No resonances that could be assigned to pyrophosphate were observed upfield of these peaks.

MjGC also hydrolyzes dGTP to form Fapy deoxyribonucleotide monophosphate (0.025 U/mg) and it hydrolyzes β,γ-methylene-GTP (0.13 U/mg) or GTP-γ-S (0.11 U/mg) to form Fapy nucleotide monophosphate, demonstrated by anion exchange chromatography and fluorogenic derivatization of the reaction products. MjGC incubated with N^7-methyl-GTP has a low activity (0.035 U/mg) in forming a ring-opened nucleotide monophosphate and inorganic phosphate. Enzymatic reactions with inosine 5′-triphosphate (ITP) form a nucleotide monophosphate that has a UV absorbance maximum at 259 nm. Derivatization of the ITP hydrolysis product formed a fluorescent compound with an excitation maximum at 395 nm and an emission maximum at 464 nm. 8-Br-GTP, 8-azido-GTP, α,β-methylene-GTP, ATP, and XTP were not substrates for MjGC: no ring-opened compound or nucleotide monophosphate was produced during incubation with any of these compounds with enzyme.

Analyses of GTP Pyrophosphatase and GTP Phosphohydrolase Activities. A coupled enzyme assay was used to quantify pyrophosphate produced in reactions in which MjGC had completely hydrolyzed its GTP substrate (*49*). No pyrophosphate (<75 μM) was detected in reactions that produced 1.3 mM Fapy nucleotide monophosphate. However, inorganic phosphate analyses identified 2.1 ± 0.2 mol P_i per mole Fapy nucleotide monophosphate formed. The reaction progress curve in Figure 1 shows the rate of phosphate production (0.99 ± 0.08 μmol min^{-1} mg^{-1}) was approximately twice that of Fapy nucleotide monophosphate production (0.46 ± 0.02 μmol min^{-1} mg^{-1}).

Although orthophosphate is the product of MjGC phosphohydrolase activity, pyrophosphate is a likely intermediate in the reaction mechanism, by analogy to the proposed GTP

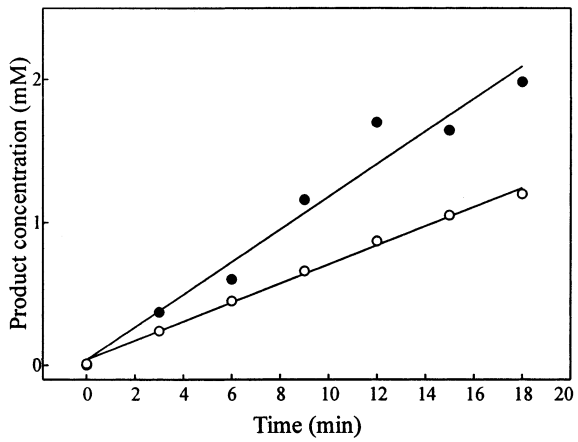

FIGURE 1: Reaction progress curve for MjGC (0.16 mg/mL) incubated with 3 mM GTP in a standard assay. Inorganic phosphate (●) and Fapy nucleotide monophosphate (○) concentrations were measured in reaction aliquots terminated with 45 mM EDTA. The average molar ratio of phosphate to Fapy nucleotide monophosphate product was 2.1:1.

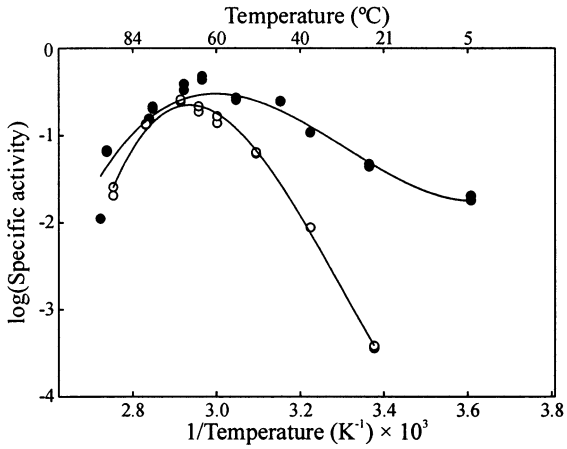

FIGURE 2: Activity versus temperature profile for MjGC. Inorganic pyrophosphate phosphohydrolase (●) and GTP cyclohydrolase (○) activities shown on this Arrhenius-type plot have comparable inflection points indicating maximum specific activity near 70 °C. Activities were measured in standard reactions at various temperatures.

cyclohydrolase II enzyme reaction mechanism. Therefore, MjGC was tested for pyrophosphate phosphohydrolase activity and was shown to hydrolyze 0.37 μmol PP_i/min/mg when incubated with 60 μM $NaPP_i$. The MjGC enzyme cleaves tripolyphosphate much more slowly, with a specific activity of 0.063 μmol P_i/min/mg. No hydrolysis of trimetaphosphate was detected. Assays of *p*-nitrophenyl phosphate hydrolysis in glycine/NaOH buffer (pH 9.5) detected no alkaline phosphatase activity (<0.04 U/mg) in a MjGC enzyme preparation.

MjGC demonstrated maximum GTP cyclohydrolase and PP_i phosphohydrolase activities from pH 8.0−9.0, buffered by 50 mM TAPS/KOH or 50 mM TES/KOH. Monovalent cations significantly affected GTP cyclohydrolase activity: large, chaotropic cations such as K^+ or NH_4^+ stimulated activity whereas small, kosmotropic cations (Li^+ and Na^+) either had little effect on activity (Na^+) or significantly inhibited the enzyme (Li^+). In reactions with insufficient concentrations of inorganic monocations, activity was stimulated by the organic cations Tris, triethanolamine, tricine, bicine, or spermidine. Acetate, chloride, or sulfate anions did not affect activity. In reactions with 50 mM TAPS/KOH (pH 8) 50 mM NH_4Cl promoted maximum activity. Thiol reductants (DTT or 2-mercaptoethanol) were required to prevent oxidation of the hydroxytriaminopyrimidine produced by the acid hydrolysis step of the derivatization reaction (*20*). However, the reductants did not stimulate MjGC GTP cyclohydrolase activity and could be added after the enzymatic reaction. To simplify the assay, 10 mM DTT was included in all GTP cyclohydrolase assays.

Divalent cation requirements were tested using MjGC enzyme, GTP, TAPS/KOH, and NH_4Cl solutions passed through a Chelex 100 column. No activity was detected in reactions without added metals, and maximum GTP cyclohydrolase activity was measured in reactions containing at least 4 mM $MgCl_2$ with 1 mM GTP. Compared to reactions containing 1 mM GTP and 5 mM $MgCl_2$ (0.59 U/mg specific activity), no other metal supported full activity at a 5 mM concentration: $MnCl_2$ (7% relative activity), $CoCl_2$ (0.6%), $NiCl_2$ (0.5%), $CuCl_2$, and $ZnSO_4$ (0.3%). Reactions containing either $CaCl_2$ or $BaCl_2$ produced no detectable amount of Fapy nucleotide monophosphate. Reactions containing both 5 mM $MgCl_2$ and 5 mM $MnCl_2$ or 5 mM $CaCl_2$ produced less than 5% of the levels of Fapy nucleotide monophosphate in reactions containing $MgCl_2$ alone. In pyrophosphate phosphohydrolase reactions using the Chelex treated MjGC, no activity was observed without added divalent cations. In reactions containing 200 μM PP_i at pH 8.0, MjGC had maximal PP_i phosphohydrolase activity in the presence of 5 mM $MgCl_2$; higher concentrations of $MgCl_2$ did not affect activity. Relative to activity with 5 mM $MgCl_2$ lower activities were measured with $CoCl_2$ (45% relative activity), $Zn(OAc)_2$ (21%), and $MnCl_2$ (8%). No activity was observed in reactions containing $CaCl_2$ or $NiCl_2$. Discrepancies between metal activation of GTP cyclohydrolase and pyrophosphate phosphohydrolase activities suggest that MjGC may have two separate metal-binding sites. Because the effective substrate for the metal-activated MjGC enzyme is probably a Mg−GTP or Mg−PP_i complex, $MgCl_2$ was included in all reactions at a fixed concentration of 10 mM (a stoichiometry of at least 3 Mg^{2+} ions per substrate molecule).

Both GTP cyclohydrolase and PP_i phosphohydrolase activities of MjGC are highest near 70 °C (Figure 2). Above 70 °C, enzyme activity decreases due to enzyme inactivation or denaturation. Similar inflection points in both curves are consistent with a single enzyme catalyzing both reactions. In contrast, *E. coli* GTP cyclohydrolase II rapidly loses activity above 60 °C (*20*). The *E. coli* inorganic pyrophosphatase is unusually thermostable although its thermoactivity has been less well-studied (*50*).

Sequence Analysis of MjGC and Site-Directed Mutation. Genomes of several euryarchaea and crenarchaea encode homologues of the MjGC gene. These genes are unique to the Archaea and are part of the previously described archaeal genomic signature (*51*). An alignment of amino acid sequences in Figure 3 shows that homologous sequences have diverged significantly (28−60% pairwise identity), yet regions of the protein are highly conserved. Comparisons of primary and predicted secondary structure suggest that the proteins have two highly diverged copies of a single

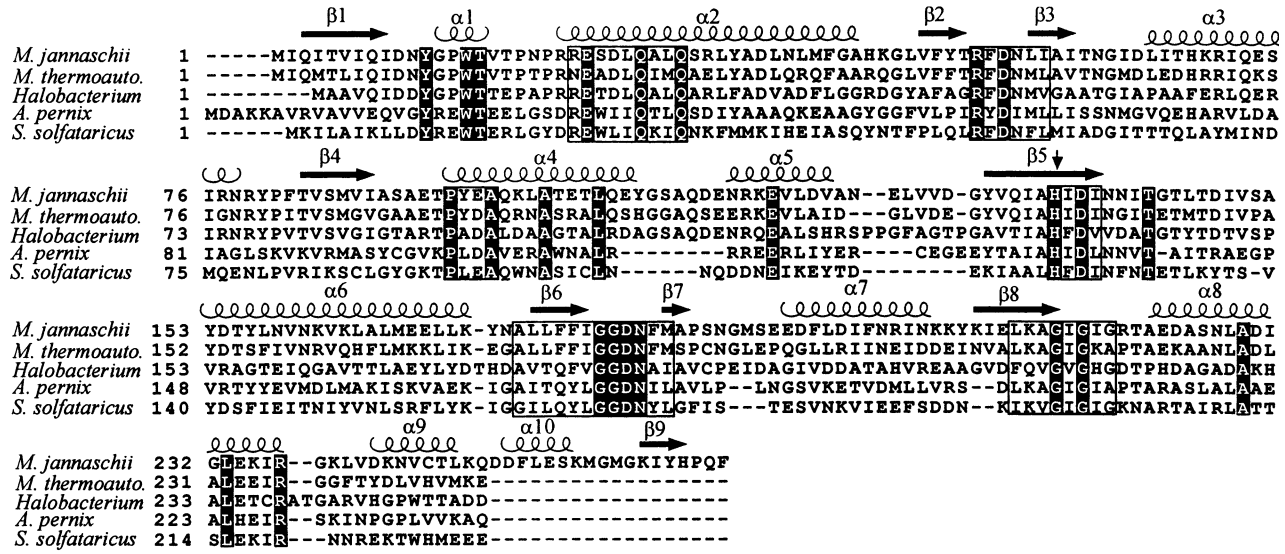

FIGURE 3: Alignment of MjGC with several archaeal homologues. Positions of identically conserved residues are shown in white on black, and regions of similarly conserved residues are boxed. Secondary structure elements were predicted for MjGC using the PHD program (*78*) and are drawn above the alignment: β-strands (arrows) and α-helices (curves). A vertical arrow indicates the conserved histidine residue that was changed in the MjGC H136Q protein. Amino acid sequences are shown for homologues from these organisms (with their respective database GenBank/EBI accession numbers): *M. jannaschii* JAL-1 (AAB98128.1), *Methanobacterium thermoautotrophicum* Δ*H* (AAB85513.1), *Halobacterium* sp. NRC-1 (AAG19434.1), *Aeropyrum pernix* K1 (BAA80359.1) and *Sulfolobus solfataricus* P2 (AAK40728.1). Sequences were aligned using the ClustalW program (*79*).

domain: MjGC residues 48−108 (β-2 through α-5) correspond to residues 179−249 (β-6 through α-9). Of particular note are conserved amino acid positions corresponding to *M. jannaschii* Glu^{24}, Asp^{55}, Glu^{96}, Glu^{119}, Asp^{138}, and Asp^{183}, which could be Mg^{2+}-coordinating ligands. Three conserved basic residues could act as hydrogen bond donors or general bases: Arg^{53}, His^{136}, or Arg^{236}. Most of these residues are located in clusters of conserved residues that may help shape the active site.

Steady-State Kinetic Analyses of MjGC Activities. To measure kinetic properties of the MjGC and MjGC−H136Q enzymes, initial reaction rates for substrate hydrolysis were measured at various substrate concentrations (Figure 4). The relevant substrates for both GTP cyclohydrolase and PP_i phosphohydrolase reactions is probably a Mg^{2+}-substrate complex; in these experiments, $MgCl_2$ was provided in excess of substrate and reactions were considered pseudo-first-order with respect to substrate. Apparent kinetic parameters for the hydrolase activities are shown in Table 2. MjGC PP_i phosphohydrolase activity is inhibited at high pyrophosphate concentrations, but no substrate or product inhibition was observed in initial rate assays of GTP cyclohydrolase activity.

To test whether the basic side chain of the one conserved histidine residue, His^{136}, is required for catalysis, we used site-directed mutagenesis to replace this amino acid with glutamine. Purified MjGC−H136Q enzyme has a much lower rate of GTP cyclohydrolase activity ($k_{cat}/K_m = 0.011$ $min^{-1}/\mu M$) relative to the wild-type enzyme ($k_{cat}/K_m = 0.39$ $min^{-1}/\mu M$) (Table 2). Likewise, its pyrophosphate phosphohydrolase activity ($k_{cat}/K_m = 0.011$ $min^{-1}/\mu M$) is low relative to wild-type enzyme ($k_{cat}/K_m = 0.16$ $min^{-1}/\mu M$). Similar to the wild-type enzyme, MjGC−H136Q produces 2.3 ± 0.4 molecules of P_i per molecule of Fapy nucleotide monophosphate. The apparent molecular mass of the mutant enzyme is equivalent to that of the wild-type enzyme, as determined by SDS-polyacrylamide gel electrophoresis. MjGC−H136Q

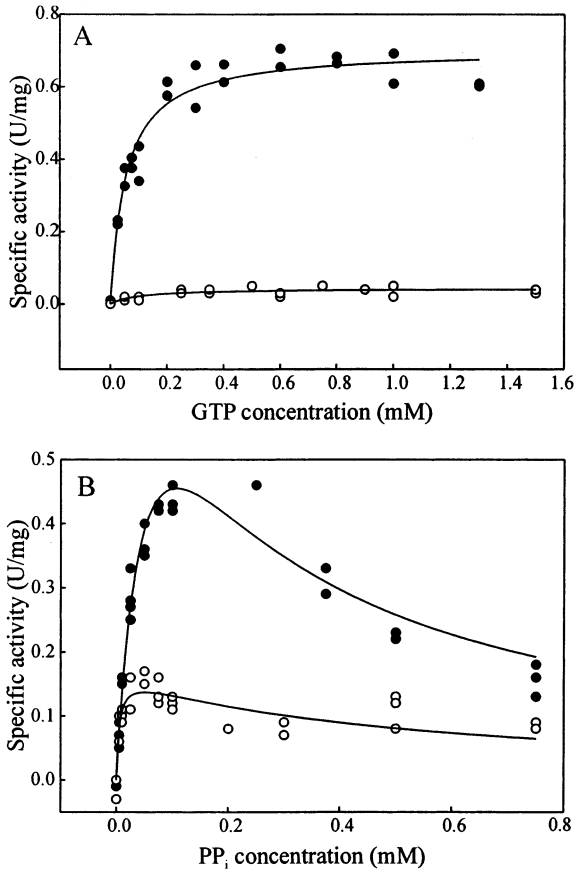

FIGURE 4: Initial rates of (A) GTP cyclohydrolase and (B) pyrophosphate phosphohydrolase activity at various substrate concentrations. Activities of wild-type MjGC (●) and mutant MjGC−H136Q (○) enzymes were measured in standard assays that included 10 mM $MgCl_2$. GTP cyclohydrolase activity data were fitted to the Henri−Michaelis−Menten equation and PP_i phosphohydrolase activity data were fitted to a simple model for substrate inhibition.

Table 2: Comparison of Apparent Kinetic Constants for GTP Cyclohydrolase and PP_i Phosphohydrolase Reactions

	GTP cyclohydrolase		PP_i phosphohydrolase		
enzyme[a]	K_m (μM)	k_{cat}[b] (min^{-1})	K_m (μM)	K_i (μM)	k_{cat}[b] (min^{-1})
GTP cyclohydrolase I	0.85 ± 0.2	1.8	n.a.[c]	n.a.	n.a.
GTP cyclohydrolase II	29 ± 3	0.9	n.a.	n.a.	n.a.
MjGC	54 ± 7	21 ± 0.5	63 ± 15	187 ± 43	30 ± 4
MjGC−H136Q	124 ± 61	1.4 ± 0.1	5.4 ± 2.3	476 ± 165	5.1 ± 0.5
soluble inorganic PP_iase	n.a.	n.a.	0.13 ± 0.06	n.a.	$23\,340 \pm 4680$

[a] Enzymes and sources of their kinetic parameters were *E. coli* GTP cyclohydrolase I (*46*), *E. coli* GTP cyclohydrolase II (*12*, *76*), MjGC and MjGC−H136Q (this work), and soluble *E. coli* inorganic pyrophosphatase (*77*). [b] Turnover numbers assume one active site per protein subunit. [c] Not applicable.

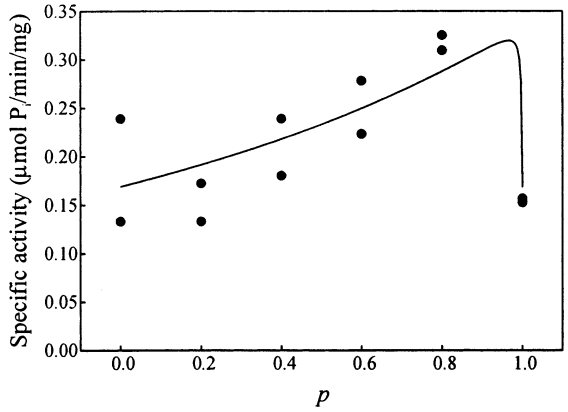

FIGURE 5: Competition plot for GTP phosphohydrolase and PP_i phosphohydrolase reactions catalyzed by MjGC. Combined initial rates of inorganic phosphate production from GTP and PPi were measured in competitive phosphohydrolase reactions (*52*, *53*). The proportion of PP_i in the reaction (p) was varied from 500 μM GTP and 0 μM PP_i ($p = 0$) to 0 μM GTP and 10 μM PP_i ($p = 1$) in standard reactions containing 10 mM $MgCl_2$ and 11 μg/mL MjGC. The data were fitted to a general model for reactions occurring at separate catalytic sites with cross-inhibition (*52*).

enzyme also has the same Stokes radius (38.1 Å) as wild-type enzyme.

Competition Assay of GTP Phosphohydrolase and PP_i Phosphohydrolase Activities. To test the relationship between GTP and PP_i phosphohydrolase activities, MjGC was incubated with various proportions of the two substrates in a competition assay (*52*, *53*). Substrate concentrations were chosen to give similar specific activities with 100% GTP (500 μM) or 100% PP_i (10 μM). A competition plot, shown in Figure 5, indicates that GTP and PP_i bind at separate sites. A model for initial rates as a function of GTP (a) and PP_i (b) substrate concentrations allowing for alternate-site inhibition was used to fit the data: $v = (V_A \times a)/(K_{mA} \times (1 + b/K_{iB}) + a) + (V_B \times b)/(K_{mB} \times (1 + a/K_{iA}) + b)$ (*52*). Parameters calculated using nonlinear regression for the data in Figure 5 were $V_A = 0.2$ μmol min^{-1} mg^{-1}, $K_{mA} = 16$ μM, $K_{iA} = 100$ μM, $V_B = 0.5$ μmol min^{-1} mg^{-1}, $K_B = 50$ μM, and $K_{iB} = 100$ μM. Differences in the limiting rates of GTP and PP_i hydrolysis could produce the observed asymmetry in the competition plot.

Inhibitors of MjGC Activity. To characterize the specificity and mechanism of this enzyme, substrate and product analogues were screened as inhibitors of MjGC GTP cyclohydrolase and PP_i phosphohydrolase activities. Potential inhibitors of GTP cyclohydrolase activity were screened in standard reactions (50 μL) containing 60 μM GTP and 0.75 μg MjGC. Neither GDP nor GMP was a substrate for GTP cyclohydrolase activity; yet less than 60% relative activity was measured in the reactions containing 60 μM concentrations of GTP and either nucleotide. Other potent inhibitors included 60 μM α,β-methylene-GTP (20%), 100 μM 8-BrGTP (50%), and 600 μM 8-azido-GTP (9%). Some moderate inhibitors were 600 μM GTP-γ-S (20% relative activity), 600 μM XTP (48%), 600 μM tripolyphosphate (50%), 600 μM IMP (75%), 600 μM orthophosphate (75%), β,γ-methylene-GTP (66%), and 600 μM methylene pyrophosphate (60%). Reactions containing 600 μM concentrations of ATP, CTP, guanosine, dGMP, xanthosine 3′-monophosphate, or trimetaphosphate retained at least 85% relative activity. Reactions containing 600 μM concentrations of methoxyamine or *O*-(4-nitrobenzyl)hydroxylamine had 84% and 77% relative activities respectively, whereas the same concentrations of hydroxylamine, *N*-methylhydroxylamine and *N*,*O*-dimethylhydroxylamine had no effect on activity.

Potential inhibitors of PP_i phosphohydrolase activity were screened in standard reactions (50 μL) containing 60 μM PP_i and 0.9 μg MjGC. Potent inhibitors included 60 μM NaF (45%), 100 μM 8-Br-GTP (46% relative activity), 300 μM 8-azido-GTP (47%), and 50 μM tripolyphosphate (48%). Moderate inhibitors included 600 μM methylene pyrophosphate (44%) and 600 μM α,β-methylene-GTP (67%). No significant inhibition was observed in reactions containing 600 μM concentrations of XTP, N^7-methyl-GTP, β,γ-methylene-GTP, GTP-γ-S, GDP, phosphoglycolate, methoxyamine, *N*-methylhydroxylamine, trimetaphosphate, or 6 mM methyl phosphate.

DISCUSSION

Two properties of MjGC distinguish it from canonical GTP cyclohydrolases. First, this enzyme hydrolyzes both $\alpha-\beta$ and $\beta-\gamma$ phosphate anhydride bonds in GTP. Because MjGC has an independent pyrophosphate phosphohydrolase activity, we propose that the enzyme removes pyrophosphate from the nucleotide substrate and subsequently hydrolyzes PP_i releasing two molecules of inorganic phosphate. Inhibitor studies, a competition assay, and metal activation profiles suggest that the GTP cyclohydrolase and PP_i phosphohydrolase activities occur at independent sites or even different enzymes. However, comparable effects on both reactions were shown by temperature profiles, mutagenesis of the MjGC His^{136} residue, and C-8 substituted GTP analogue inhibitors. Along with the lack of free PP_i in reactions, these results suggests that pyrophosphate hydrolysis occurs at an alternate site of the MjGC enzyme and is not due to low levels of a contaminating enzyme.

Pyrophosphate Hydrolysis Activities. Many other enzymes release pyrophosphate from a nucleotide 5′-triphosphate

including GTP cyclohydrolase II, DNA and RNA polymerases (*54*), aminoacyl tRNA-synthetases, nucleotidyltransferases (*55*, *56*), and nucleotide scavenging enzymes such as dUTP pyrophosphatase and members of the Nudix hydrolase family (*57*). Yet we are not aware of any other enzyme that both releases pyrophosphate from a nucleotide and hydrolyzes it to form inorganic phosphate. Pyrophosphate hydrolysis is highly exergonic due to the high solvation energy of inorganic phosphate (*58*), but most PP_i-producing enzymes leave that reaction to a separate inorganic pyrophosphate phosphohydrolase enzyme. All organisms, including *M. jannaschii*, have this essential, ubiquitous enzyme (*59*, *60*). These soluble PP_i phosphohydrolases are Mg^{2+}-dependent enzymes that use evolutionarily conserved aspartate and glutamate residues as ligands for metal ions (*60*−*62*). Although MjGC and its homologues have a similar set of conserved acidic residues, they have no sequence similarity to either family of characterized PP_i phosphohydrolases. MjGC has a much lower turnover number for PP_i hydrolysis than does the *E. coli* inorganic pyrophosphatase (Table 2). Still, this partial reaction is unlikely to be a rate-limiting step in the complete GTP cyclohydrolase reaction.

Implications of the Formylaminopyrimidine Product. The second distinguishing feature of MjGC is its release of a formylaminopyrimidine product, Fapy nucleotide monophosphate. Reaction mechanisms of both GTP cyclohydrolases I and II necessarily include a formylaminopyrimidine intermediate that is reversibly formed by opening the imidazole ring of guanine (*19*, *21*). In both canonical enzymes, the guanine ring opens rapidly compared to the rates of substrate binding, intermediate rearrangement and release. Although these formylaminopyrimidine compounds are quite stable, wild-type enzymes do not release them (*21*, *46*). Archaea that have homologues of MjGC presumably have another enzyme that hydrolyzes Fapy nucleotide monophosphate to produce the triaminopyrimidine substrate for flavin and neopterin biosyntheses (*63*, *64*). Because formylaminopyrimidine is a common product of oxidative damage to guanine bases in both free nucleotides and nucleic acid polymers, the cells must have a scavenging system to prevent accumulation and incorporation of this mutagenic nucleotide into new RNA and DNA (*65*, *66*).

Nucleotide Substrate Recognition. The substrate specificity of MjGC suggests that the enzyme discriminates among bases by recognizing the 2-amino and 6-oxo purine substituents of the guanine base. ITP, which lacks the 2-amino group of GTP, is a substrate for MjGC. Nevertheless, XTP, a 2-oxo analogue of GTP, is not a substrate, and it inhibits GTP cyclohydrolase activity. Besides interfering with hydrogen bonding, replacing a 2-amino group with a 2-oxo group dramatically lowers the molecule's pK_a from 9.2 (guanosine) to 5.7 (xanthosine). The distributed negative charge on XTP could prevent nucleophilic attack at the C-8 position (*67*). Replacing the 6-oxo group of ITP with the 6-amino group of ATP also produces an inactive substrate. Many enzymes use a hydrogen-bond donating residue to discriminate between GTP and ATP (*68*). While the N^7-methyl-GTP imidazole ring spontaneously opens rapidly compared to GTP (*28*, *69*), MjGC catalyzes the hydrolysis of the alkylated purine more slowly than GTP. Perhaps by disrupting a hydrogen bond between the protein (or a water molecule) and the 7-imino position of guanine, the alkyl substituent of N^7-methyl-GTP slows binding to form a productive enzyme−substrate complex.

Substituents of the ribose moiety of GTP are also crucial for productive substrate binding. The 2′-hydroxyl of GTP may be a hydrogen bond donor: dGTP is hydrolyzed to Fapy deoxyribonucleotide monophosphate more slowly than GTP. Finally, a 5′-triphosphate group is required for activity: GMP is not a substrate, even in the presence of exogenous pyrophosphate. As ligands to Mg^{2+}, these phosphate groups could be required to correctly position a $Mg(OH)^+$ complex for nucleophilic attack at the C-8 position of GTP, bound to the enzyme in the anti conformation.

Toward an Enzymatic Reaction Mechanism. The reaction catalyzed by MjGC most likely involves Mg^{2+}-dependent deprotonation of water, producing hydroxide nucleophiles at several sites (*70*, *71*). The order of these hydrolysis reactions remains to be determined. It is not yet clear whether the pyrophosphatase activity (release of pyrophosphate) precedes the hydrolytic opening of the imidazole ring. Neither do we know how MjGC couples pyrophosphate phosphohydrolysis to the ring-opening reaction, significantly improving the turnover of MjGC relative to GTP cyclohydrolase I and II enzymes (Table 2).

The nonenzymatic alkaline hydrolysis of purine derivatives suggests a model for the GTP cyclohydrolase reaction mechanism (*72*, *73*). A nucleophilic hydroxide ion attacks C-8 of the imidazole ring to generate a tetrahedral intermediate, which rearranges to the formamide. Alternatively, the hydroxide ion attack could be facilitated by the initial protonation of N-7. Hydrolysis of the resulting imidazolinium cation has been documented for imidazoline model compounds (*74*), $N^{5,10}$-methenyltetrahydrofolate (*75*) and N^7-methyl-GTP (*28*, *69*). We expect that future studies of the enzyme's structure will help to elucidate this enzyme's complex mechanism and evolution. Because MjGC has a faster turnover and greater protein thermostability than GTP cyclohydrolase II, genetically engineered strains containing a member of this novel family, and a formylaminopyrimidine hydrolase enzyme could produce higher riboflavin yields in large-scale fermentation processes.

ACKNOWLEDGMENT

We thank Dr. Marion Graupner for screening alternative genes for GTP cyclohydrolase activity. We thank Tom Glass at the Analytical Services facility (Virginia Tech Department of Chemistry) for assistance with NMR and Dr. Mehdi Ashraf-Khorassani (Virginia Tech Department of Chemistry) for performing APCI-MS analysis.

REFERENCES

1. White, R. H. (1991) Distribution of folates and modified folates in extremely thermophilic bacteria, *J. Bacteriol. 173*, 1987−1991.
2. White, R. H. (1986) Biosynthesis of the 7-methylated pterin of methanopterin, *J. Bacteriol. 165*, 215−218.
3. Keller, P. J., Floss, H. G., Le Van, Q., Schwarzkopf, B., and Bacher, A. (1986) Biosynthesis of methanopterin in *Methanobacterium thermoautotrophicum*, *J. Am. Chem. Soc. 108*, 344−345.
4. Wuebbens, M. M., and Rajagopalan, K. V. (1995) Investigation of the early steps of molybdopterin biosynthesis in *Escherichia coli* through the use of *in vivo* labeling studies, *J. Biol. Chem. 270*, 1082−1087.
5. Johnson, J. L., Rajagopalan, K. V., Mukund, S., and Adams, M. W. W. (1993) Identification of molybdopterin as the organic

component of the tungsten cofactor in four enzymes from hyperthermophilic Archaea, *J. Biol. Chem. 268*, 4848−4852.
6. Jaenchen, R., Schönheit, P., and Thauer, R. K. (1984) Studies on the biosynthesis of coenzyme F_{420} in methanogenic bacteria, *Arch. Microbiol. 137*, 362−365.
7. Eisenreich, W., Schwarzkopf, B., and Bacher, A. (1991) Biosynthesis of nucleotides, flavins, and deazaflavins in *Methanobacterium thermoautotrophicum*, *J. Biol. Chem. 266*, 9622−9631.
8. Kuchino, Y., Kasai, H., Nihei, K., and Nishimura, S. (1976) Biosynthesis of the modified nucleoside Q in transfer RNA, *Nucleic Acids Res. 3*, 393−398.
9. Bai, Y., Fox, D. T., Lacy, J. A., Van Lanen, S. G., and Iwata-Reuyl, D. (2000) Hypermodification of tRNA in thermophilic archaea: cloning, over-expression, and characterization of tRNA-guanine transglycosylase from *Methanococcus jannaschii*, *J. Biol. Chem. 275*, 28731−28738.
10. Dufton, M. J., Gibson, C. L., Pitt, A. R., Athmani, S., and Suckling, C. J. (1997) On the mechanism of action of GTP-transforming enzymes, *Bioorg. Med. Chem. Lett. 7*, 779−784.
11. Nar, H., Huber, R., Auerbach, G., Fischer, M., Hosl, C., Ritz, H., Bracher, A., Meining, W., Eberhardt, S., and Bacher, A. (1995) Active site topology and reaction mechanism of GTP cyclohydrolase I, *Proc. Natl. Acad. Sci. U.S.A. 92*, 12120−12125.
12. Ritz, H., Schramek, N., Bracher, A., Herz, S., Eisenreich, W., Richter, G., and Bacher, A. (2001) Biosynthesis of riboflavin: studies on the mechanism of GTP cyclohydrolase II, *J. Biol. Chem. 276*, 22273−22277.
13. Bult, C. J., White, O., Olsen, G. J., Zhou, L., Fleischmann, R. D., Sutton, G. G., Blake, J. A., FitzGerald, L. M., Clayton, R. A., Gocayne, J. D., Kerlavage, A. R., Dougherty, B. A., Tomb, J.-F., Adams, M. D., Reich, C. I., Overbeek, R., Kirkness, E. F., Weinstock, K. G., Merrick, J. M., Glodek, A., Scott, J. L., Geoghagen, N. S. M., Smith, H. O., Woese, C. R., and Venter, J. C. (1996) Complete genome sequence of the methanogenic archaeon, *Methanococcus jannaschii*, *Science 273*, 1017−1140.
14. Burg, A. W., and Brown, G. M. (1968) The biosynthesis of folic acid. 8. Purification and properties of the enzyme that catalyzes the production of formate from carbon atom 8 of guanosine triphosphate, *J. Biol. Chem. 243*, 2349−2358.
15. Auerbach, G., Herrmann, A., Bracher, A., Bader, G., Gutlich, M., Fischer, M., Neukamm, M., Garrido-Franco, M., Richardson, J., Nar, H., Huber, R., and Bacher, A. (2000) Zinc plays a key role in human and bacterial GTP cyclohydrolase I, *Proc. Natl. Acad. Sci. U.S.A. 97*, 13567−13572.
16. Shiota, T., Palumbo, M. P., and Tsai, L. (1967) A chemically prepared formamidopyrimidine derivative of guanosine triphosphate as a possible intermediate in pteridine biosynthesis, *J. Biol. Chem. 242*, 1961−1969.
17. Schramek, N., Bracher, A., Fischer, M., Auerbach, G., Nar, H., Huber, R., and Bacher, A. (2002) Reaction mechanism of GTP cyclohydrolase I: single turnover experiments using a kinetically competent reaction intermediate, *J. Mol. Biol. 316*, 829−837.
18. Bracher, A., Eisenreich, W., Schramek, N., Ritz, H., Götze, E., Herrmann, A., Gütlich, M., and Bacher, A. (1998) Biosynthesis of pteridines. NMR studies on the reaction mechanisms of GTP cyclohydrolase I, pyruvoyltetrahydropterin synthase, and sepiapterin reductase, *J. Biol. Chem. 273*, 28132−28141.
19. Schramek, N., Bracher, A., and Bacher, A. (2001) Ring opening is not rate-limiting in the GTP cyclohydrolase I reaction, *J. Biol. Chem. 276*, 2622−2626.
20. Foor, F., and Brown, G. M. (1975) Purification and properties of guanosine triphosphate cyclohydrolase II from *Escherichia coli*, *J. Biol. Chem. 250*, 3545−3551.
21. Schramek, N., Bracher, A., and Bacher, A. (2001) Biosynthesis of riboflavin. Single turnover kinetic analysis of GTP cyclohydrolase II, *J. Biol. Chem. 276*, 44157−44162.
22. van Loon, A. P. G. M., Hohmann, H.-P., Bretzel, W., Hümbelin, M., and Pfister, M. (1996) Development of a fermentation process for the manufacture of riboflavin, *Chimia 50*, 410−412.
23. Hümbelin, M., Griesser, V., Keller, T., Schurter, W., Haiker, M., Hohmann, H.-P., Ritz, H., Richter, G., Bacher, A., and van Loon, A. (1999) GTP cyclohydrolase II and 3,4-dihydroxy-2-butanone-4-phosphate synthase are rate-limiting enzymes in riboflavin synthesis of an industrial *Bacillus subtilis* strain used for riboflavin production, *J. Ind. Microbiol. Biotech. 22*, 1−7.
24. Hyman, A. A., Salser, S., Drechsel, D. N., Unwin, N., and Mitchison, T. J. (1992) Role of GTP hydrolysis in microtubule dynamics: information from a slowly hydrolyzable analogue, GMPCPP, *Mol. Biol. Cell 3*, 1155−1167.
25. Lee, P., Gorrell, A., Fromm, H. J., and Colman, R. F. (1999) 8-(4-Bromo-2,3-dioxobutylthio)guanosine 5′-triphosphate: a new affinity label for purine nucleotide sites in proteins, *Arch. Biochem. Biophys. 372*, 205−213.
26. Dunn, D. B., and Hall, R. H. (1970) Purines, pyrimidines, nucleosides and nucleotides: physical constants and spectral properties in *Handbook of Biochemistry*: *Selected Data for Molecular Biology* (Sober, H. A., Ed.) Vol. pp G3-G238, Chemical Rubber Co., Cleveland, OH.
27. *Specifications and Criteria for Biochemical Compounds* (1972) National Academy of Sciences, Washington, DC.
28. Hendler, S., Furer, E., and Srinivasan, P. R. (1970) Synthesis and chemical properties of monomers and polymers containing 7-methylguanine and an investigation of their substrate or template properties for bacterial deoxyribonucleic acid or ribonucleic acid polymerases, *Biochemistry 9*, 4141−4153.
29. Graham, D. E., Xu, H., and White, R. H. (2002) Identification of coenzyme M biosynthetic phosphosulfolactate synthase. A new family of sulfonate-biosynthesizing enzymes, *J. Biol. Chem. 277*, 13421−13429.
30. Graham, D. E., Xu, H., and White, R. H. (2002) *Methanococcus jannaschii* uses a pyruvoyl-dependent arginine decarboxylase in polyamine biosynthesis, *J. Biol. Chem. 29*, 29.
31. Combs, M. T., Ashraf-Khorassani, M., and Taylor, L. T. (1999) HPLC/atmospheric pressure chemical ionization-mass spectroscopy of eight regulated sulfonamides, *J. Pharm. Biomed. Anal. 19*, 301−308.
32. Pfleiderer, W. (1985) Chemistry of naturally ocurring pterins in *Folates and Pterins*: *Chemistry and Biochemistry of Pterins* (Blakley, R. L., and Benkovic, S. J., Eds.) Vol. 2, pp 43−114, John Wiley & Sons, New York.
33. Richter, G., Ritz, H., Katzenmeier, G., Volk, R., Kohnle, A., Lottspeich, F., Allendorf, D., and Bacher, A. (1993) Biosynthesis of riboflavin: cloning, sequencing, mapping, and expression of the gene coding for GTP cyclohydrolase II in *Escherichia coli*, *J. Bacteriol. 175*, 4045−4051.
34. Graupner, M., and White, R. H. (2001) Biosynthesis of the phosphodiester bond in coenzyme F_{420} in the methanoarchaea, *Biochemistry 40*, 10859−10872.
35. Itaya, K., and Ui, M. (1966) A new micromethod for the colorimetric determination of inorganic phosphate, *Clin. Chim. Acta 14*, 361−366.
36. Cogan, E. B., Birrell, G. B., and Griffith, O. H. (1999) A robotics-based automated assay for inorganic and organic phosphates, *Anal. Biochem. 271*, 29−35.
37. Bessey, O. A., Lowry, O. H., and Brock, M. J. (1946) A method for the rapid determination of alkaline phosphatase with five cubic millimeters of serum, *J. Biol. Chem. 164*, 321−329.
38. Poyner, R. R., Cleland, W. W., and Reed, G. H. (2001) Role of metal ions in catalysis by enolase: an ordered kinetic mechanism for a single substrate enzyme, *Biochemistry 40*, 8009−8017.
39. Cleland, W. W. (1979) Substrate inhibition, *Methods Enzymol. 63*, 500−513.
40. Smith, D. R., Doucette-Stamm, L. A., Deloughery, C., Lee, H., Dubois, J., Aldredge, T., Bashirzadeh, R., Blakely, D., Cook, R., Gilbert, K., Harrison, D., Hoang, L., Keagle, P., Lumm, W., Pothier, B., Qiu, D., Spadafora, R., Vicaire, R., Wang, Y., Wierzbowski, J., Gibson, R., Jiwani, N., Caruso, A., Bush, D., Safer, H., Patwell, D., Prabhakar, S., McDougall, S., Shimer, G., Goyal, A., Pietrokovski, S., Church, G. M., Daniels, C. J., Mao, J.-I., Rice, P., Nölling, J., and Reeve, J. N. (1997) Complete genome sequence of *Methanobacterium thermoautotrophicum* ΔH: functional analysis and comparative genomics, *J. Bacteriol. 179*, 7135−7155.
41. Galagan, J. E., Nusbaum, C., Roy, A., Endrizzi, M. G., Macdonald, P., FitzHugh, W., Calvo, S., Engels, R., Smirnov, S., Atnoor, D., Brown, A., Allen, N., Naylor, J., Stange-Thomann, N., DeArellano, K., Johnson, R., Linton, L., McEwan, P., McKernan, K., Talamas, J., Tirrell, A., Ye, W., Zimmer, A., Barber, R. D., Cann, I., Graham, D. E., Grahame, D. A., Guss, A. M., Hedderich, R., Ingram-Smith, C., Kuettner, H. C., Krzycki, J. A., Leigh, J. A., Li, W., Liu, J., Mukhopadhyay, B., Reeve, J. N., Smith, K., Springer, T. A., Umayam, L. A., White, O., White, R. H., Conway de Macario, E., Ferry, J. G., Jarrell, K. F., Jing, H., Macario, A. J., Paulsen, I., Pritchett, M., Sowers, K. R., Swanson, R. V., Zinder, S. H., Lander, E., Metcalf, W. W., and Birren, B. (2002) The genome of *M. acetivorans* reveals extensive metabolic and physiological diversity, *Genome Res. 12*, 532−542.

42. Overbeek, R., Fonstein, M., D'Souza, M., Pusch, G. D., and Maltsev, N. (1999) The use of gene clusters to infer functional coupling, *Proc. Natl. Acad. Sci. U.S.A. 96*, 2896−2901.
43. Graham, D. E., and White, R. H. (2002) Elucidation of methanogenic coenzyme biosyntheses: from spectroscopy to genomics, *Nat. Prod. Rep. 19*, 133−147.
44. Choi, K.-P., Bair, T. B., Bae, Y.-M., and Daniels, L. (2001) Use of transposon Tn*5367* mutagenesis and a nitroimidazopyran-based selection system to demonstrate a requirement for *fbiA* and *fbiB* in coenzyme F_{420} biosynthesis by *Mycobacterium bovis* BCG, *J. Bacteriol. 183*, 7058−7066.
45. Graupner, M., Xu, H., and White, R. H. (2002) Characterization of the 2-phospho-L-lactate transferase enzyme involved in coenzyme F_{420} biosynthesis in *Methanococcus jannaschii*, *Biochemistry 41*, 3754−3761.
46. Bracher, A., Fischer, M., Eisenreich, W., Ritz, H., Schramek, N., Boyle, P., Gentili, P., Huber, R., Nar, H., Auerbach, G., and Bacher, A. (1999) Histidine 179 mutants of GTP cyclohydrolase I catalyze the formation of 2-amino-5-formylamino-6-ribofuranosylamino-4(*3H*)-pyrimidinone triphosphate, *J. Biol. Chem. 274*, 16727−16735.
47. Kenne, L., Unger, P., and Wehler, T. (1988) Synthesis and nuclear magnetic resonance studies of some *N*-acylated methyl 4-amino-4,6-dideoxy-α-D-mannopyranosides, *J. Chem. Soc., Perkins Trans. 1988*, 1183−1186.
48. Schendel, F. J., Cheng, Y. S., Otvos, J. D., Wehrli, S., and Stubbe, J. (1988) Characterization and chemical properties of phosphoribosylamine, an unstable intermediate in the de novo purine biosynthetic pathway, *Biochemistry 27*, 2614−2623.
49. O'Brien, W. E. (1976) A continuous spectrophotometric assay for argininosuccinate synthetase based on pyrophosphate formation, *Anal. Biochem. 76*, 423−430.
50. Josse, J., and Wong, S. C. K. (1971) Inorganic pyrophosphatase of Escherichia coli in *The Enzymes* (Boyer, P. D., Ed.) Vol. 4, pp 499−527, Academic Press, New York.
51. Graham, D. E., Overbeek, R., Olsen, G. J., and Woese, C. R. (2000) An archaeal genomic signature, *Proc. Natl. Acad. Sci. U.S.A. 97*, 3304−3308.
52. Chevillard, C., Cárdenas, M. L., and Cornish-Bowden, A. (1993) The competition plot: a simple test of whether two reactions occur at the same active site, *Biochem. J. 289*, 599−604.
53. Cárdenas, M. L. (2001) The competition plot: A kinetic method to assess whether an enzyme that catalyzes multiple reactions does so at a unique site, *Methods 24*, 175−180.
54. Holm, L., and Sander, C. (1995) DNA polymerase β belongs to an ancient nucleotidyltransferase superfamily, *Trends Biochem. Sci. 20*, 345−347.
55. Brenner, C. (2002) Hint, Fhit, and GalT: function, structure, evolution, and mechanism of three branches of the histidine triad superfamily of nucleotide hydrolases and transferases, *Biochemistry 41*, 9003−9014.
56. Brown, K., Pompeo, F., Dixon, S., Mengin-Lecreulx, D., Cambillau, C., and Bourne, Y. (1999) Crystal structure of the bifunctional *N*-acetylglucosamine 1-phosphate uridyltransferase from *Escherichia coli*: a paradigm for the related pyrophosphorylase superfamily, *EMBO J. 18*, 4096−4107.
57. Bessman, M. J., Frick, D. N., and O'Handley, S. F. (1996) The MutT proteins or "Nudix" hydrolases, a family of versatile, widely distributed, "housecleaning" enzymes, *J. Biol. Chem. 271*, 25059−25062.
58. George, P., Witonsky, R. J., Trachtman, M., Wu, C., Dorwart, W., Richman, L., Richman, W., Shurayh, F., and Lentz, B. (1970) "Squiggle-H_2O". An enquiry into the importance of solvation effects in phosphate ester and anhydride reactions, *Biochim. Biophys. Acta 223*, 1−15.
59. Kuhn, N. J., Wadeson, A., Ward, S., and Young, T. W. (2000) *Methanococcus jannaschii* ORF mj0608 codes for a class C inorganic pyrophosphatase protected by Co^{2+} or Mn^{2+} ions against fluoride inhibition, *Arch. Biochem. Biophys. 379*, 292−298.
60. Sivula, T., Salminen, A., Parfenyev, A. N., Pohjanjoki, P., Goldman, A., Cooperman, B. S., Baykov, A. A., and Lahti, R. (1999) Evolutionary aspects of inorganic pyrophosphatase, *FEBS Lett. 454*, 75−80.
61. Samygina, V. R., Popov, A. N., Rodina, E. V., Vorobyeva, N. N., Lamzin, V. S., Polyakov, K. M., Kurilova, S. A., Nazarova, T. I., and Avaeva, S. M. (2001) The structures of *Escherichia coli* inorganic pyrophosphatase complexed with Ca^{2+} or $CaPP_i$ at atomic resolution and their mechanistic implications, *J. Mol. Biol. 314*, 633−645.
62. Ahn, S., Milner, A. J., Fütterer, K., Konopka, M., Ilias, M., Young, T. W., and White, S. A. (2001) The "open" and "closed" structures of the type-C inorganic pyrophosphatases from *Bacillus subtilis* and *Streptococcus gordonii*, *J. Mol. Biol. 313*, 797−811.
63. Graupner, M., Xu, H., and White, R. H. (2002) The pyrimidine nucleotide reductase step in riboflavin and F_{420} biosynthesis in archaea proceeds by the eukaryotic route to riboflavin, *J. Bacteriol. 184*, 1952−1957.
64. Howell, D. M., and White, R. H. (1997) D-*erythro*-neopterin biosynthesis in the methanogenic archaea *Methanococcus* [*sic*] *thermophila* and *Methanobacterium thermoautotrophicum* ΔH, *J. Bacteriol. 179*, 5165−5170.
65. Wiederholt, C. J., and Greenberg, M. M. (2002) Fapy•dG Instructs Klenow Exo^- to Misincorporate Deoxyadenosine, *J. Am. Chem. Soc. 124*, 7278−7279.
66. Pouget, J.-P., Douki, T., Richard, M. J., and Cadet, J. (2000) DNA damage induced in cells by γ and UVA radiation as measured by HPLC/GC-MS and HPLC-EC and Comet assay, *Chem. Res. Toxicol. 13*, 541−549.
67. Stoychev, G., Kierdaszuk, B., and Shugar, D. (2002) Xanthosine and xanthine: substrate properties with purine nucleoside phosphorylases, and relevance to other enzyme systems, *Eur. J. Biochem. 269*, 4048−4057.
68. Nobeli, I., Laskowski, R. A., Valdar, W. S., and Thornton, J. M. (2001) On the molecular discrimination between adenine and guanine by proteins, *Nucleic Acids Res. 29*, 4294−4309.
69. Townsend, L. B., and Robins, R. K. (1963) Ring cleavage of purine nucleosides to yield possible biogenic precursors of pteridines and riboflavin, *J. Am. Chem. Soc. 85*, 242−243.
70. Herschlag, D., and Jencks, W. P. (1990) Catalysis of the hydrolysis of phosphorylated pyridines by $Mg(OH)^+$: a possible model for enzymatic phosphoryl transfer, *Biochemistry 29*, 5172−5179.
71. Katz, A. K., Glusker, J. P., Markham, G. D., and Bock, C. W. (1998) Deprotonation of water in the presence of carboxylate and magnesium ions, *J. Phys. Chem. B 102*, 6342−6350.
72. Lönnberg, H., Lukkari, J., and Lehikoinen, P. (1982) Mechanisms for the solvolytic decompositions of nucleoside analogs. IX. Pathways for the alkaline hydrolysis of 6-substituted 9-(1-alkoxyethyl)purines, *Acta Chem. Scand., Ser. B 36*, 707−712.
73. Lönnberg, H., Lukkari, J., and Lehikoinen, P. (1984) Mechanisms for the solvolytic decompositions of nucleoside analogues. XII. Further studies on the alkaline hydrolysis of 9-(1-alkoxyethyl)-purines, *Acta Chem. Scand., Ser. B 38*, 573−578.
74. DeWolfe, R. H. (1975) Kinetics and mechanisms of reactions of amidines, in *The Chemistry of Amidines and Imidates* (Patai, S., Ed.) Vol. 1, pp 349−384, John Wiley & Sons, New York.
75. Robinson, D. R., and Jencks, W. P. (1967) Mechanism and catalysis of the hydrolysis of methyltetrahydrofolic acid, *J. Am. Chem. Soc. 89*, 7098−7103.
76. Bacher, A., Richter, G., Ritz, H., Eberhardt, S., Fischer, M., and Krieger, C. (1997) Biosynthesis of riboflavin: GTP cyclohydrolase II, deaminase, and reductase, *Methods Enzymol. 280*, 382−389.
77. Avaeva, S. M., Rodina, E. V., Kurilova, S. A., Nazarova, T. I., and Vorobyeva, N. N. (1996) Effect of D42N substitution in Escherichia coli inorganic pyrophosphatase on catalytic activity and Mg^{2+} binding, *FEBS Lett. 392*, 91−94.
78. Rost, B., and Sander, C. (1994) Combining evolutionary information and neural networks to predict protein secondary structure, *Proteins 19*, 55−72.
79. Thompson, J. D., Higgins, D. G., and Gibson, T. J. (1994) CLUSTAL W: improving the sensitivity of progressive multiple sequence alignment through sequence weighting, position-specific gap penalties and weight matrix choice, *Nucleic Acids Res. 22*, 4673−4680.

BI0268798